IOP Conf. Series: Journal of Physics: Conf. Series **842** (2017) 012056 doi:10.1088/1742-6596/842/1/012056

Study on observation condition and on simple evaluation method of TypeIV creep damage of Mod.9Cr-1Mo steel

F Kawashima[1] , T Masumitsu[2], K Negi[3], K Watanabe[3] and K Fujiwara[1]

[1] Faculty of Advanced Science and Technology, Kumamoto University
2-39-1 Kurokami, Chuoku, Kumamoto 860-8555, Japan
[2] Graduate School of Science and Technology, Kumamoto University
[3] Department of Mechanical Engineering, Faculty of Engineering, Kumamoto University

E-mail: kawashima@mech.kumamoto-u.ac.jp

Abstract. Type IV creep damage is the phenomena that a large number of voids in micron size initiate, grow, coalesce each other and become large cracks. They initiate in welded joints of high chromium steel in power plant. The density of voids, the number of voids per a unit area, is used to evaluate the residual life. The observed density of voids depends on the observation conditions; the observation area and the magnification of observed photograph of metallographic structure, because voids do not distribute uniformly and the small magnification misses the small voids. In previous study, we studied the influence of them with simulated fine-grain HAZ of Mod.9Cr-1Mo steel, and proposed how to determine the appropriate observation area for the temporary allowable error. We also proposed the method to evaluate the start time of initiation of voids, the initiation rate of voids and the growth rate of voids based on the relation between the observed density of voids and the magnification. But the experimental data was short. In this paper we showed new data, but they were yet not sufficient. We used FEM analysis and considered why enough data had been not taken.

1. Introduction

Type IV creep damage is the phenomena that a large number of voids in micron size initiate, grow, coalesce and become large cracks[1]. They initiate in the fine grain heat affected zone (FGHAZ) in the welded joints that have been exposed to stress and high temperature for years. For reliable use of power plants, the method to evaluate the residual life is demanded. The density of voids is defined as the number of voids per a unit area. It is used as the parameter of the life fraction of the component with Type IV creep damage[2]. The observed density of voids depends on the observation conditions[3] which are the observation area and the magnification of observed photograph of metallographic structure, because voids do not distribute uniformly and the small magnification misses the small voids.

Generally Type IV creep damage initiates under high stress triaxiality. However the influence of the stress and the stress triaxiality on the density of voids has been researched[4][5], the quantitative conclusion has not been taken yet. One of the reasons is that the influence of the stress and stress triaxiality is hidden by the influence of the observation conditions. In the previous research[6][7][8], authors proposed the method to determine the appropriate observation area. They showed that the influence of the Heat on the appropriate observation areas was small.

In the previous research[7] the linear relation between the mean density of voids and the reciprocal of the magnification also was taken. There was the probability that the relation represents the distribution of the radius of voids. The initiation rate, the growth rate and the start time of initiation of voids might be evaluated with the distribution of the radius. However, data were short to discuss it. In this research we add data and try to evaluate these parameters and to calculate the density of voids. However, they are not enough, either. We use FEM analysis and consider the reason of short data.

2. Materials, creep test and observation

The creep tests were conducted with simulated FGHAZ and the samples with Type IV creep damage were obtained.

The material was KA SFVAF28, which was forged Mod.9Cr-1Mo steel. Table 1 shows the chemical composition of this material. It was normalized at 1045 C for 3.5 hours and tempered at 760 C for 5.5 hours. After that it was cut to the bars. To reproduce the metallographic structure of FGHAZ, the Heat 1 and the Heat 2 were heated at 910 C for 1 second one time and three times, respectively. After that the test pieces were machined from the bars.

To simulate the Post Weld Heat Treatment (PWHT), and to remove the residual strain, the test pieces were heated for 2 hours at 740 C after the machining. Table 2 shows the Vickers hardness measured with 9.807N and the average grain size after PWHT.

Tests were conducted with notched test pieces and a smooth test piece. Figure 1 (a) shows the notched test piece of Heat 1 with M18 screws. The shape of smooth test piece of Heat 1 was the same as figure 1 except for the notch. Figure 1 (b) shows the notched test piece of Heat 2 with M14 screws. The net section stress of the notched test pieces of the Heat 1, the smooth test piece of Heat 1 and the notched test pieces of Heat 2 were 72.8 MPa, 40.6 MPa and 44.2 MPa, respectively.

The test temperature was 650 C. The fracture time of notched test piece of Heat 1 and that of Heat 2 were 1487 hours and 2302 hours, respectively. The smooth test piece of Heat 1 didn't fracture and the notch factor is unknown. The similar notched test pieces need from 1.3 to 1.4 times larger net section stress to the same fracture time as the smooth test piece[9].

The stress and *TF*, the triaxiality factor, were analyzed with FEM with ANSYS Academic Teaching Introductory. Young's modulus of 157 GPa and Poisson's ratio of 0.314 were used. Equation (1) is the used Norton's law. TF is defined with equation (2).

$$\dot{\varepsilon} = 4.3270\times10^{-15}\sigma^{5.8143} \quad [\text{hour}^{-1},\ \text{MPa}]\ , \tag{1}$$

where $\dot{\varepsilon}$ is creep rate and σ is stress.

$$TF = \frac{(\sigma_1 + \sigma_2 + \sigma_3)}{\sigma_{mises}}\ . \tag{2}$$

Table 1 Chemical composition. [%]

	C	Si	Mn	P	S	Ni	Cr	Mo	V	Nb
Heat 1	0.10	0.30	0.45	0.014	0.001	0.16	9.34	0.96	0.21	0.07
Heat 2	0.11	0.30	0.45	0.015	0.001	0.18	9.16	0.96	0.23	0.07

Table 2 Hardness and grain size.

	Hardness [HV][a]	Grain size [μm]
Heat 1	225	2.23[b]
Heat 2	235	4.22[c]

[a] measured with 9.807N
[b] Observed with the magnification of 2520
[c] Observed with the magnification of 2544

For the example, figure 2 (a) and (b) show the distributions of stress and *TF* on the cross section of the bottom of the notch, respectively. They distribute uniformly in the area with the radius of less than 1 mm, and we observed this area. The creep damage of the centre of this cross section (radius r=0 mm) and that of the bottom of the notch (r=3.75 mm) were calculated with the time fraction rule shown with equation (3).

$$D_C = \Sigma\left(\frac{t_{\mathrm{i}}}{t_{\mathrm{ri}}}\right), \tag{3}$$

where D_C, t_{i} and t_{ri} are the creep damage, the period during that the principal stress is σ_{i} and the creep fracture time for σ_{i}. t_{ri} is calculated with equations (4) and (5).

$$LMP = (T + 273.15)(\log_{10} tr + 20)\ . \tag{4}$$

$$\log_{10}\sigma = -2.143\times10^{-4} LMP + 6.282\ . \tag{5}$$

The creep damages are shown in figure 3. It was evaluated that the test piece fractures when the damage of bottom of the notch is 1. The creep damage at the centre is approximately 0.3 when the test piece fractures. The reason of the small observed density of voids may be that the creep damage of observed area was small.

Figure 4 shows the observed cross sections. Table 3 shows the test time, the stress and *TF* of the observed cross section. Only the cross section f was on the smooth test piece. Other cross sections were on notched test pieces.

The cross sections were etched with Nital. Figure 5 shows the example of metallographic structure. The observed photographs of metallographic structure were taken and printed with a optical microscope, a digital camera and a printer. The magnification of them, O, were approximately 1000, 500 and 250.

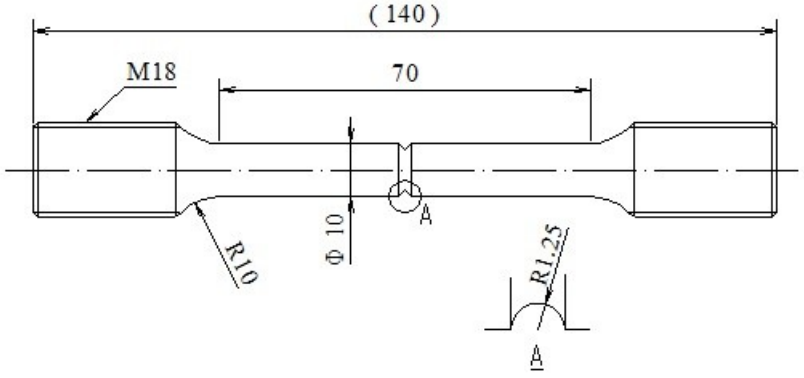

(a)

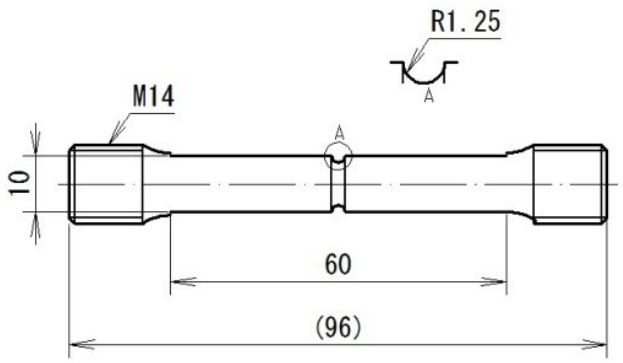

(b)

Figure 1 Notched test piece. (a) and (b) are Heat 1 and Heat 2, respectively.

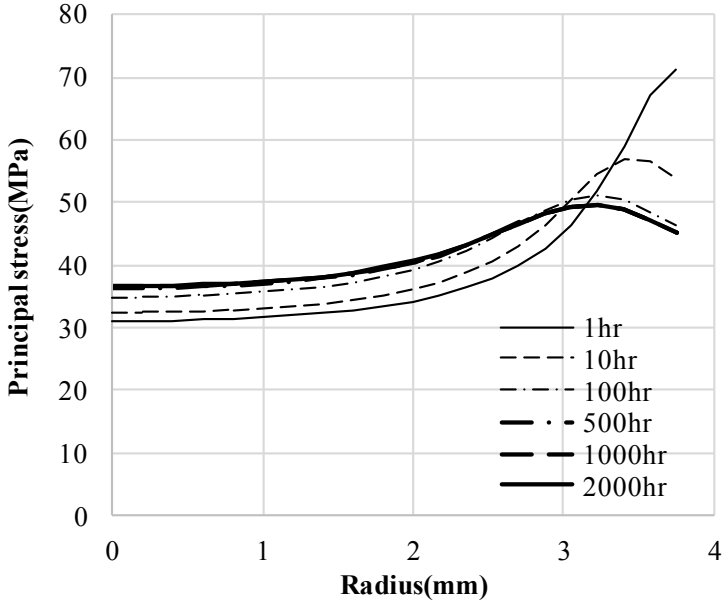

(a)

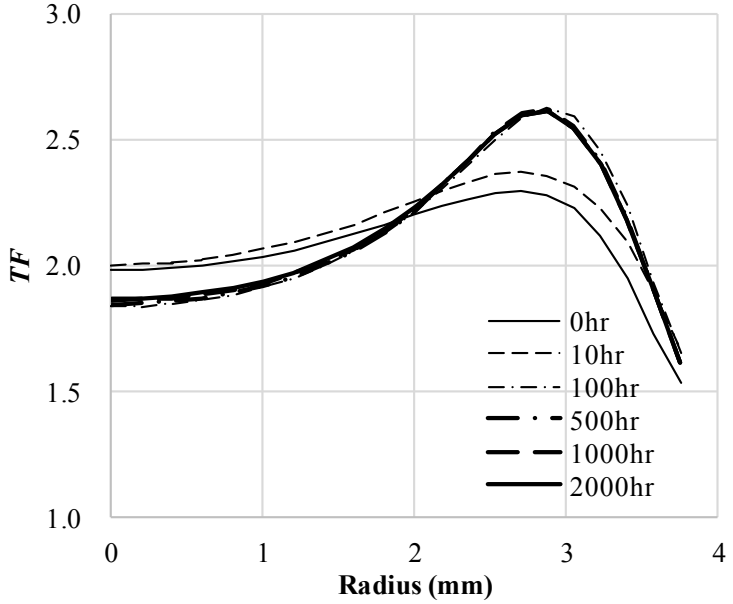

(b)

Figure 2 Stress and *TF* distribution on cross section of the bottom of notch. (a) and (b) are stress distribution and *TF* distribution, respectively.

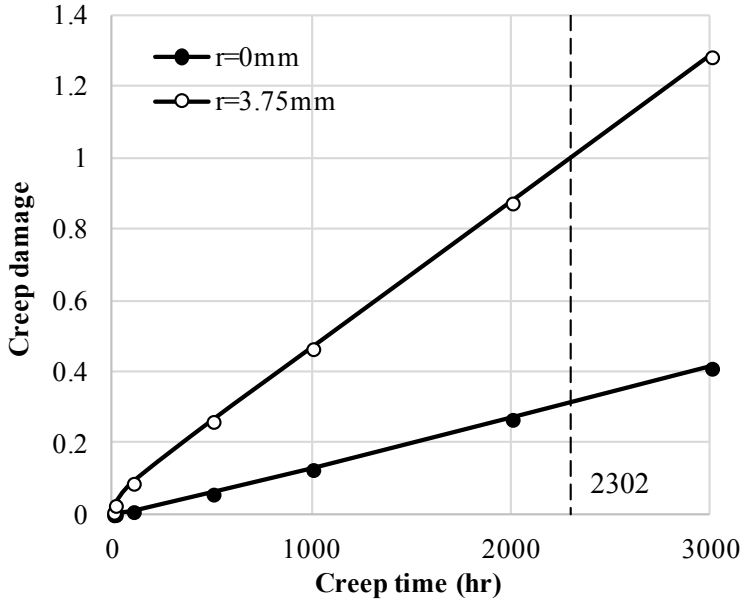

Figure 3 Creep damage of the observed area and the bottom of the notch.

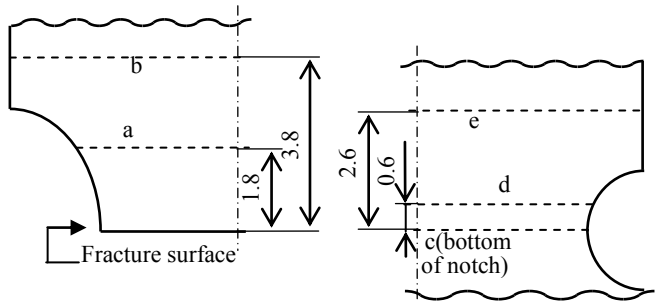

(a)

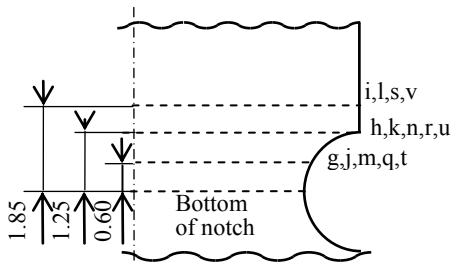

(b)

Figure 4 Outline of observed cross sections. (a) and (b) are Heat 1 and Heat 2, respectively.

Table 3 Observed cross section.

Heat	Test Piece	Cross Section	Time (hr)	Y [b] (mm)	S or N[c]	σ_1 (MPa)	*TF*
1	2	a	1487[a]	1.80	N	65.6	1.9
		b		3.80	S	53.9	1.2
	3	c	1353	0	N	62.6	1.9
		d		0.60	N	63.4	2.0
		e		2.60	S	63.2	1.6
	4	f	1242	-	S	40.6	1.0
2	2-3	g	2072	0.60	N	37.4	1.9
		h		1.25	N	38.5	1.9
		i		1.85	S	39.0	1.8
	2-4	j	2181	0.60	N	37.4	1.9
		k		1.25	N	38.5	1.9
		l		1.85	S	39.0	1.8
	2-5	m	2279	0.60	N	37.4	1.9
		n		1.25	N	38.5	1.9
		p		2.06	S	-	-
	2-7	q	2281	0.60	N	37.4	1.9
		r		1.25	N	38.5	1.9
		s		1.85	S	39.0	1.8
	2-8	t	2163	0.60	N	37.4	1.9
		u		1.25	N	38.5	1.9
		v		1.85	S	39.0	1.8

[a] Fracture time
[b] Distance from the cross section of bottom of notch after the test
[c] N: Notched part, S: Smooth part

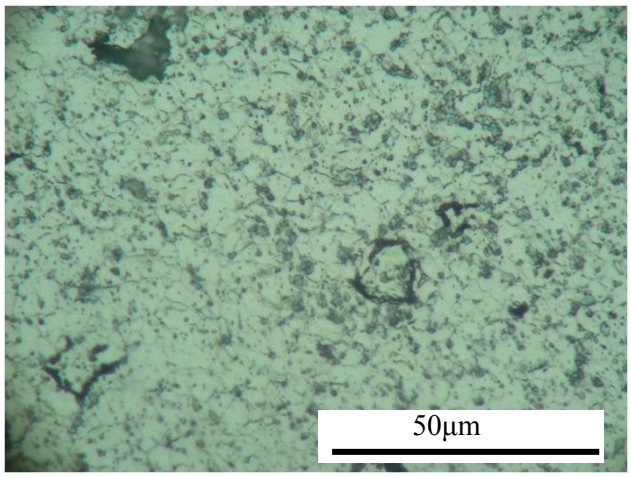

Figure 5 The metallographic structure of cross section.

The pictures were connected to be the circle with the radius of 1mm where the stress distributed uniformly (figure 6). The circle was divided to rectangles. A is the area of each rectangles. Except for cross section a and b, A is 0.04mm^2 when O is 500 or 1000 and 0.08mm^2 when O is 250, respectively. In cross section a, A is 0.10mm^2, 0.07mm^2 and 0.06mm^2 when O is 250, 500 and 1000, respectively. In cross section b, A is 0.09mm^2 when O is 250 and 0.04mm^2 when O is 500 or 1000. Figure 7 shows the examples.

The size of observed area, s, is the same as A, or is twice or four times as large as A. i is the density of voids of each s. The distribution of i was taken. The mean and the standard deviation of i are represented with i_u and i_s, respectively.

Figure 6 Observed metallographic photograph of cross section a.

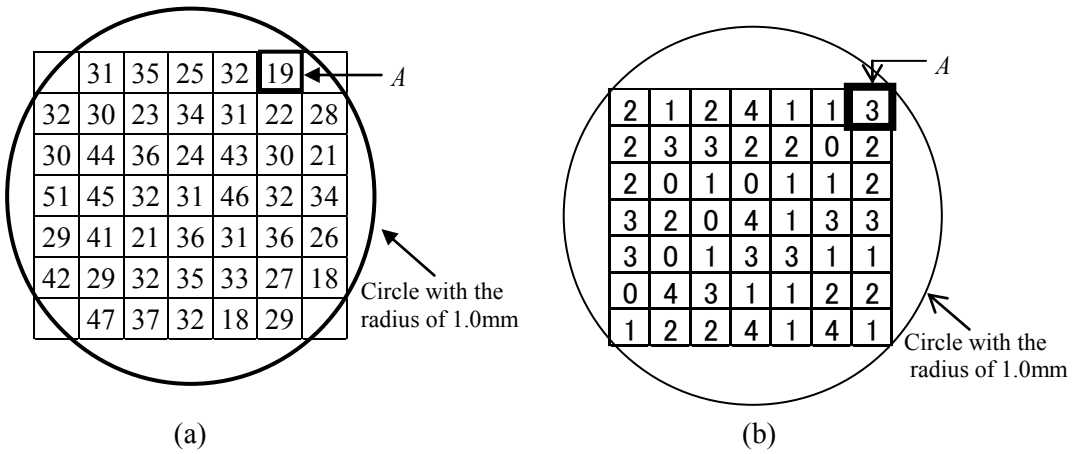

(a) (b)

Figure 7 Distribution of the number of voids.
(a) and (b) are cross section a and cross section n, respectively.

3. Results of observation

Figure 8 shows the example of $F(i)$ that is the cumulative distribution of i. Their approximating curves are normal distributions. i_s is small if s is large.

The allowable error of i should be determined based on the allowable error of the evaluated life fraction. But the relation between i and the life fraction is unknown. We assumed the allowable error of $0.8i_u \le i \le 1.2i_u$. Figure 9 is the relation between the density of voids i and the confidence level $F(1.2i_u) - F(0.8i_u)$ that is the probability of i being in the allowable error. Figure 10 shows that the confidence level increases with the increase of s. The area appropriate for the confidence level of 0.8 is shown in figure 11. It is function of i_u. The grain size of Heat 2 is about twice as large as that of the Heat 1, and the summation of grain boundary length per unit area of Heat 2 is shorter than that of Heat 1. But, in figure 11, there is not the difference between the Heat 1 and Heat 2. The reason may be that at the same i_u the influence of the grain size is cancelled.

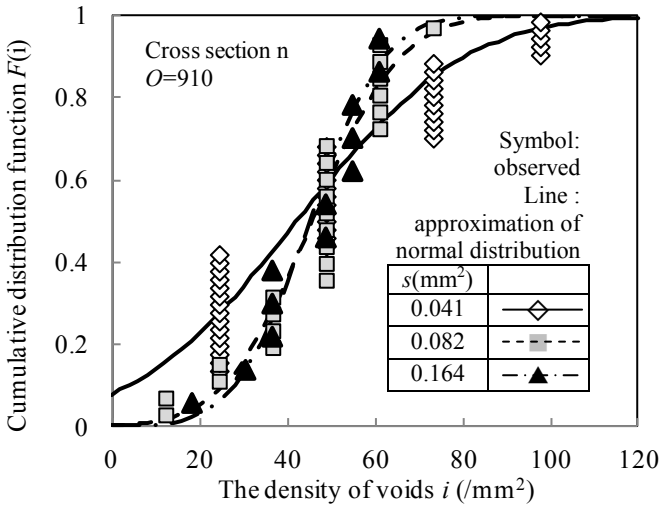

Figure 8 Cumulative distribution Function of density of voids (cross section n, O =910)

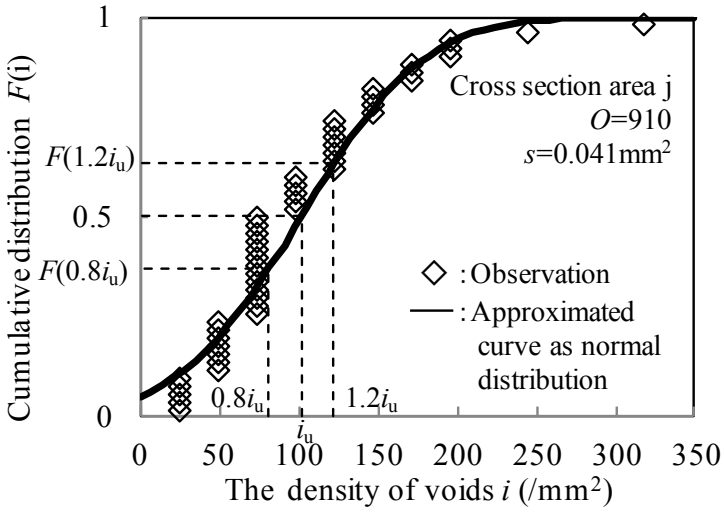

Figure 9 Outline of confidence level (cross section j, O=910).

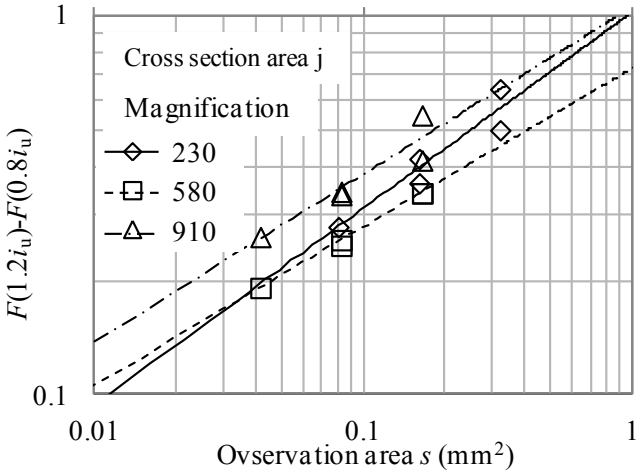

Figure 10 Relation of confidence level $F(1.2i_u) - F(0.8i_u)$ and observation area s .

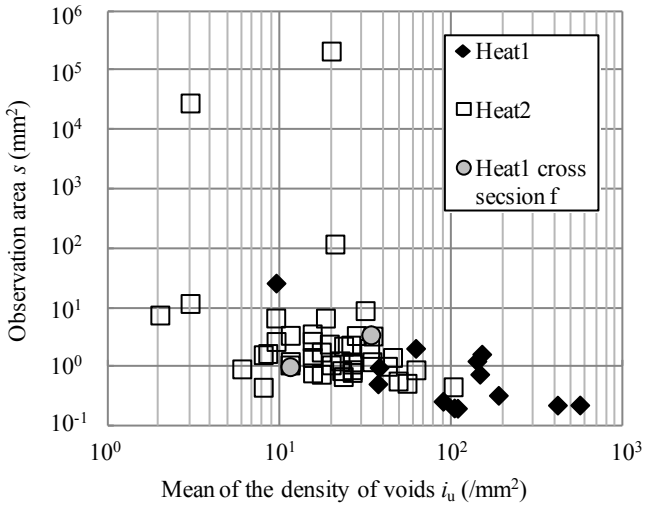

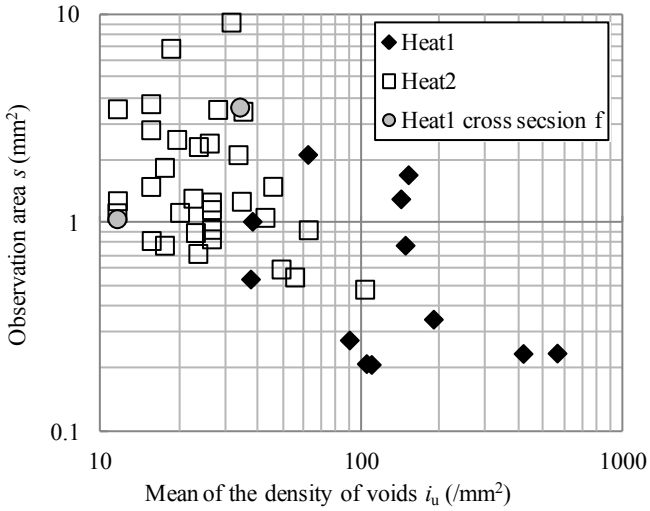

Figure 11 Range of appropriate observation conditions.
(a) shows all data. (b) shows data in practical range.

4. Evaluation method of initiation and growth of voids

Figure 12 shows the relation between O and i_u. Figure 12 (a) shows the cross sections of Heat 1 observed with 3 magnifications. Figure 12 (b) shows the cross sections of Heat 2 with the distance of 1.85mm from the bottom of notch. i_u seems to be linear to the reciprocal of O except for cross section l. There seemed to be some failures in observation of cross section l.

The minimum radius that one can see by the naked eyes is assumed to be ρ. In the photograph with the magnification of O, the voids with radius larger than ρ/O can be observed. Therefore the relation between O and i_u shows the distribution of the radiuses of voids.

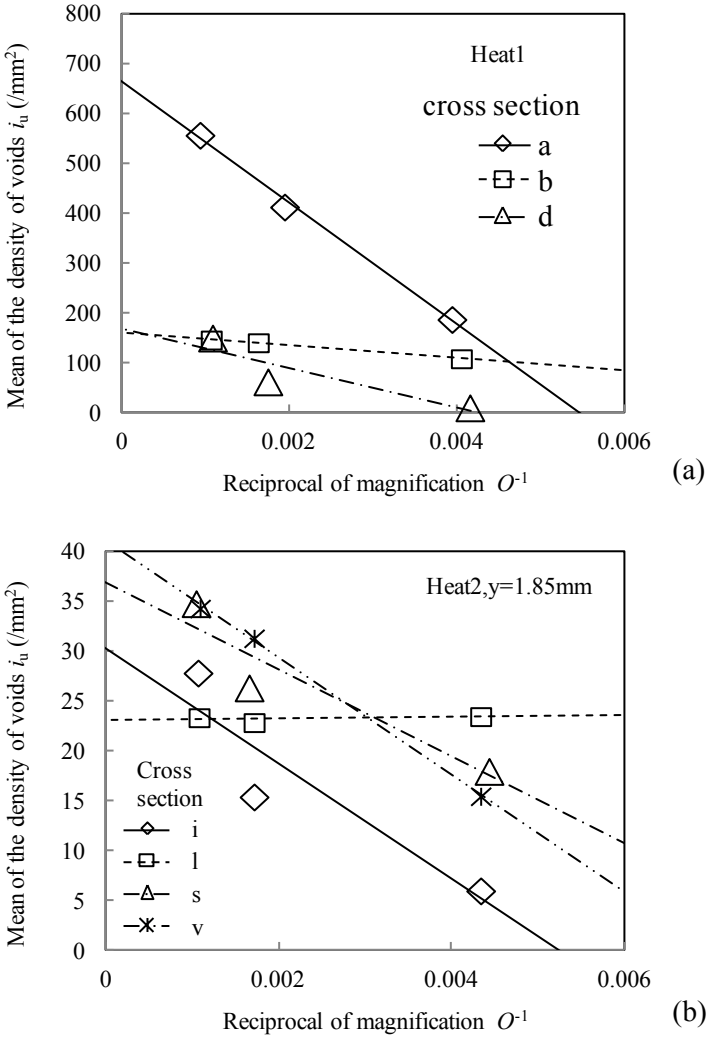

Figure 12 Relation between mean of density of voids i_u and reciprocal of magnification O^{-1}. (a) shows the cross sections of Heat 1 observed with more than three magnifications. (b) shows the cross sections with the distance of 1.85 mm from bottom of notch.

It is assumed that voids start to initiate at t_1. The initiation rate and the growth rate of voids are assumed to be the functions of time; $G(t)$ mm^{-2}hour^{-1} and $H(t)$ mm hour^{-1}, respectively. The radius of voids that initiates at t_o becomes $r = \int_{t_0}^{t_2} H(t)dt$ at t_2. And the density of voids with radius larger than $r = \int_{t_0}^{t_2} H(t)dt$ is $i = \int_{t_1}^{t_0} G(t)dt$ at t_2.

If the initiation rate and the growth rate are constant, $G(t) = f$ and $H(t) = h$, then the relation become $r = h(t_2 - t_0)$ and $i = f(t_0 - t_1)$. Equation (6) is made of these two equations. It shows the density of voids $i(r,t)$ whose radius are larger than r at the time of t.

$$i(r,t) = -\frac{f}{h}r + f(t - t_1) \quad , \tag{6}$$

where r, t, f, h, and t_1 represent the radius of void (mm), the creep time (hour), the voids' initiation rate (hour^{-1} mm^{-2}), the voids' growth rate (mm hour^{-1}) and the time at that the voids' initiation started (hour), respectively. $r = \rho/O$ is substituted into equation (6), then equation (6) becomes equation (7).

$$i(r,t) = -\frac{f}{h/\rho}O^{-1} + f(t - t_1) \, . \tag{7}$$

In equation (7), i is linear to O^{-1}. It corresponds to the observation. $-\frac{f}{h/\rho}$ and $f(t - t_1)$ in equation (7) are the slope and axial section of figure 12.

Perhaps there are $G(t)$ and $H(t)$ that are not constant [10][11][12][13] [14] [15] and correspond to the observation, but in this research we use the simple assumption.

As shown in table 3 and figure 3, cross section i, s and v are in the same location; 1.85 mm from bottom of the notch. The stress of these cross sections is same. So we assume that f, h and t_1 of these cross sections are same. This assumption is valid because the slopes of them in figure 12 (b) are almost the same. Observed i_u and the creep time of the three cross sections are substituted into $i(r,t)$ and t in equation (7), and f, h and t_1 are calculated with the least squares method. Also f, h and t_1 of the other cross sections of Heat 2 that are 0.6 mm and 1.25 mm from bottom of the notch are calculated. Data of test piece 2-4 (cross section j, k, l) are not used for the calculation because the relations between i_u and O^{-1} are irregular. Table 4 shows the results. The density of voids calculated with equation (7) and the variables in table 4 are compared to the observation in figure 13. Errors of observation are large. The reason of that is thought to be not enough observation area. In this study observation area of i_u is about 2 mm^2, which is the area of the largest square in circle with radius of 1 mm. As shown in figure 11, because i_u of Heat 2 is small, observation area might be need more than 2 mm^2.

Table 4 Estimated start time of initiation t_1, initiation rate f and growth rate h.

y[a] (mm)	t_1 (hour)	f (/mm^2/hr)	h/ρ (/hr)
0.6	1317	4.783×10^{-2}	9.214×10^{-6}
1.25	1384	5.220×10^{-2}	6.021×10^{-6}
1.85	1446	4.510×10^{-2}	11.30×10^{-6}

[a] Distance from bottom of notch after the test

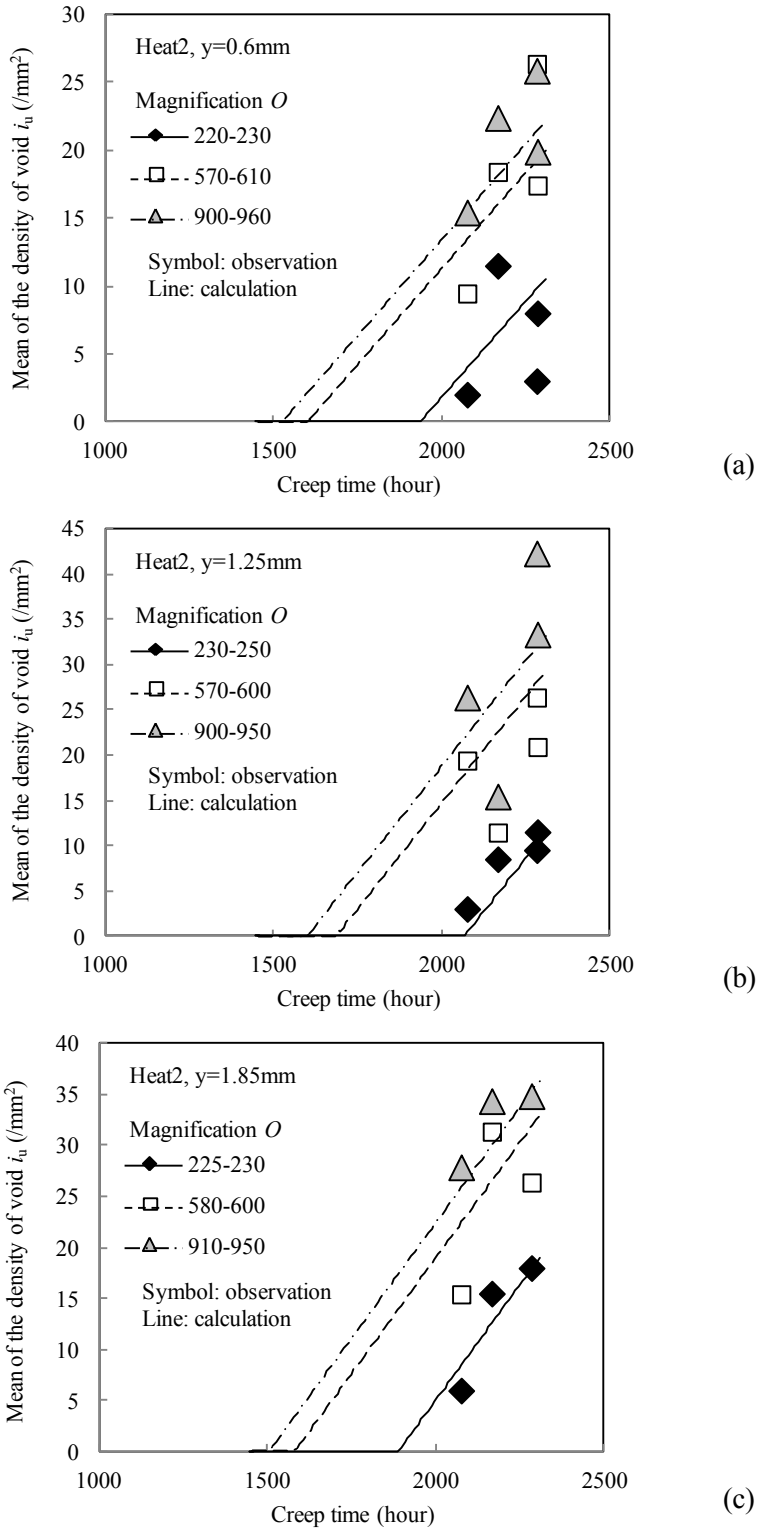

Figure 13 Calculated density of voids compared with the test results. (a), (b) and (c) show the cross sections with y of 0.6 mm, 1.25 mm, and 1.85 mm, respectively.

Though there is the error, equation (7) well expresses the relation of i_u and O^{-1}. So the calculated variables are thought to be valid.

It is not clear whether there are differences among variables of three cross sections. In the next test, we should use the test piece with the observation areas with various *TF* or observation areas of high creep damage (in other words, large density of voids) at fracture time.

In some conditions, i_u might not be liner to O^{-1}. In that case we should study $G(t)$ and $H(t)$ that are not constant but functions of time.

5. Conclusions

The observation area appropriate for the assumed allowable error of $0.8i_u \le i \le 1.2i_u$ with the confidence level of 0.8 is determined. The appropriate area is small if the density of voids is large. The influence of Heat on the appropriate area is thought to be small.

The method that estimates the voids' initiation rate, growth rate and the initiation start time is proposed. It needs the observation more than two times with more than two magnifications. This method will be used to estimate the influence of *TF* on Type IV creep damage.

References

[1] Ellis F. V and Viswanathan R 1998 Review of type IV cracking *ASME-PVP* **380** 59-76

[2] Xu Qihua, Xu Qiang, Lu Z and Donnelly S 2013 The development of phisical-base creep damage constitutive equation for P/T22 (2.25Cr-1Mo) steel at low stress *Proc. of 6th International 'HIDA' Conference* S4B-03

[3] The Iron and Steel Institute of Japan 1991 *Manual on evaluation of creep-fatigue damage / lives by replication method* (Tokyo: The Iron and Steel Institute of Japan) Japan 28-33

[4] Fujimoto M, Sakane M, Date S and Yoshida H 2005 Multiaxial creep rupture and damage evaluation for 2.25Cr-1Mo forged steel *Jour. of the Society of Materials Science*, *Japan* Japan **54** 2 149-54

[5] Himeno T, Chuman Y, Tokiyoshi T, Fukahori T and Igari T 2013 Creep rapture behanior of girth-welded mod. 9Cr-1Mo steel pipe subject to internal pressure and axial load *Proc. of 6th Int. 'HIDA' Conf.* (Nagasaki: 2-4 December, 2013 / European Technology Development) S6-05

[6] Kawashima F, Kinoshita T, Sato A, Enui Y, Fujiwara K and Hata H 2013 Experimental research on the appropriate extent of observation area of creep voids to evaluate the remaining life of Mod.9Cr-1Mo steel with Type IV creep damage *Proc. of 6th Int. 'HIDA' Conf.* (Nagasaki: 2-4 December, 2013 / European Technology Development) S2-02

[7] Kawashima F, Sato A, Irie Y, Yamakawa K, Fujiwara K and Hata H 2015 Study on the observation condition of Type IV creep damage of Mod. 9Cr-1Mo steel *Proc. of the 1st Int. Conf. on Advanced High-Temperature Materials Technology for Sustainable and Reliable Power Engineering (123HiMAT-2015)* (Sapporo: 29 June - 3 July, 2015 / 123 Comitte on Heat Resisting Materials and Alloys, Japan Society for thr Promotion of Science) 82-85

[8] Kawashima F, Sato A, Irie Y, Yamakawa K, Fujiwara K and Hata H 2015 Study on the magnification and area of observation appropriate to measure Type IV creep damage of Mod.9Cr-1Mo steel *Jour. of the Society of Materials Science,Japan* Japan **64** 74-79

[9] Takahashi Y 2009, Creep rapture behavior of modified 9Cr-1Mo steel under multiaxial stress and its modeling, *Jour. of the Society of Materials Science*, *Japan* Japan **58** 2 115-21

[10] Raj R and Ashby M. F 1975 Intergranular Fracture at elevated temperature *Acta Metallurgica* **23** 653-66

[11] Raj R 1978 Nucleation of cavities at second phase particles in grain boundaries *Acta Metallurgica* **26** 995-1006

[12] Chuang T-J, Kagawa K. I, Rice J. R and Sills L. B 1979 Non-equibrium models for diffuseive cavities of grain intefaces *Acta Metallurgica* **27** 265-84

[13] Pharr G. M and Nix W. D 1979 A nimerical study of cavity growth controlled by surface diffusion *Acta Metallurgica* **27** 1615-31
[14] Rice J. R 1981 Constraints on the diffusive cavitation of isolated grain boundary facets on creeping polycrystals *Acta Metallurgica* **29** 675-81
[15] Nix W. D, Yu K. S and Wang J. S 1983 The effect of segregation on the kinetics of intergranular cavity growth under creep conditions *Metallurgical and Materials Trans*. A **14** 563-70